

X-Ray and Far-uv Photoemission from Amorphous and Crystalline Films of Se and Te

N. J. Shevchik, M. Cardona, and J. Tejeda

Max-Planck-Institut für Festkörperforschung, Stuttgart, Federal Republic of Germany

(Received 2 April 1973)

Photoemission experiments have been performed on amorphous and crystalline films of Se and Te using photon excitation energies of 1486.6 (AlK α), 40.8, and 21.2 eV (He II and He I). From these experiments we have determined the densities of valence states, the binding energies of the core levels, the characteristic loss functions, and the plasma frequencies. Comparisons of the experimental to the theoretical densities of states are made for both the amorphous and crystalline forms. The optical properties of Te in the region of interband transitions are shown to be described well by a simple model based on the density of valence states. Evidence that the optical absorption peak from the Se 3d level may be of excitonic origin is presented.

I. INTRODUCTION

The electronic properties of the crystalline and amorphous modifications of Se and Te have been the object of much interest.¹⁻³ However, in spite of the vast accumulation of experimental work, the properties of the amorphous forms are still not well understood. The lack of long-range order makes the computation of the electronic spectra prohibitively difficult without introducing simplified models.⁴⁻⁷ The results of band-structure calculations for both the amorphous and crystalline phases have been usually tested by comparison to the experimental optical constants.⁴⁻¹⁵ Such comparisons are not conclusive tests since alterations in the valence bands, the conduction bands, or the transition probabilities can produce the necessary adjustments needed to fit the experimental optical results. A more direct test of a calculated electronic spectrum is obtained by comparing the theoretical to the experimental density of the valence states, since here only a single rather than a joint density of states is involved.

Photoemission employing both x-ray and uv photons is the ideal tool to determine the density of valence states of the two structural forms. Experiments performed with high-energy photons ($h\nu > 20$ eV) permit the density of valence states to be examined without the complicating effects of final states. However, with the use of the limited resolution of x-ray photoemission (~ 0.5 eV at best, even with a crystal monochromator),¹⁶ the finer features of the density of states cannot be seen. The use of uv photoemission permits resolutions of 0.1 eV and better to be attained, allowing the finer features of the density of valence states to be resolved.^{17,18} Because of the effects of secondary electrons and transition matrix elements, the lower portions of the valence band (more than 10 eV below the top) may not always be seen with uv photoemission, whereas they are usually easily observed with x-ray excitation. The

combined use of both x-ray and uv photoemission allows a composite density of states to be derived which retains the best features of each method of excitation.

Another advantage of employing the x-ray photoemission is that the core levels may also be studied. Accurate determination of the energy of core levels provides a means to investigate the charge transferred by an element upon forming compounds and to determine the nature of optical absorption processes from deep-lying core levels. Unfortunately, many of the previously reported core levels¹⁹ have been measured with reference to the Fermi energies of the samples, which may vary as much as the band gap, and the effects of charging introduce additional uncertainties into these measurements. By determining the positions of the core levels with respect to the top of the valence band, both the effects of charging and uncertainties in the Fermi level can be eliminated. In addition, such determinations need not rely upon calibration of the Fermi level of the spectrometer.

Earlier photoemission experiments on Se and Te have been performed with photons of low energy so that only the top 3 eV of the valence bands were observed.²⁰⁻²² Also with such low energies, the effects of final states can still be important. More recent measurements of Nielsen,²³ with 21.2-eV photons, permitted the top portions of the amorphous form of Se to be observed, but the lower s bands were not resolved. X-ray photoemission measurements on trigonal Te gave the entire valence-band density of states,¹⁶ but the resolution (0.5 eV) was not sufficient to bring out any sharper structure that may have existed.

Here we present x-ray and uv photoemission data for both the amorphous and crystalline forms of Se and Te. From these data, we have determined the densities of valence states, the positions of the core levels with respect to the top of the valence band, and the characteristic energy loss functions. The density of valence states will be

compared to those calculated for both the amorphous and crystalline forms. Also, we compare the experimental optical spectrum of Te in the visible and near uv with a model calculated from the experimental density of valence states. The far-uv absorption spectrum of Se corresponding to transitions from the $3d$ core levels yields, in conjunction with photoemission data for the core level, evidence for final-state ("exciton") interaction in this absorption process. Similar results are reported for the $4d$ absorption edge of Te.

II. STRUCTURE

Se and Te belong to group VI in the Periodic Table. Characteristic of elements in this row is their tendency to have twofold coordination in their elemental forms. In their trigonal crystalline forms, the atoms are arranged in spiral chains oriented along the c axis. These chains are located at the center and six corners of a hexagon. The bonding angles are 105.5° and 102.6° for Se and Te, respectively. Se can also be found in α and β monoclinic forms, in which Se_8 rings form the basic structural unit. Te, however, is found only in the trigonal chainlike structure.

Amorphous Se, as recently reviewed by Adler,³ is most likely composed of chains and Se_8 rings in relative proportions that may depend upon the deposition conditions. In the amorphous form, the nearest-neighbor bonds retain the lengths of the crystalline forms. Little information is available about the structure of amorphous Te. Koma *et al.*²⁴ conclude from nuclear-magnetic-resonance experiments that the amorphous form consists of chains of 10 atoms in length, with unsatisfied bonds terminating the ends of the chains, in agreement with the fact that Te forms no crystalline phases with ring structures.

III. BAND THEORY

As discussed by Tutihasi and Chen⁹ we should expect the density of states of Se and Te to consist of three main peaks. Two electrons per atom fill the deepest-lying s -like levels. The remaining four electrons fill the p orbitals: two of them form lone-pair bonds, while the remaining two pair spins with electrons on the nearest neighbors to form bands. We expect the electrons participating in bonds to lie lower in energy than the lone-pair electrons since they are repelled by the empty antibonding states.

The primitive cell in the trigonal crystalline forms contains three atoms. We thus expect each of the atomic orbitals to split into three bands making a total of nine bands. The p -like part of the band structure of Se and Te with its antibonding, the lone-pair, and bonding components, have been discussed in a pedagogically pleasing paper

by Reitz.⁸ Since this work, many others have followed,⁹⁻¹⁵ including the pseudopotential calculations by Sandrock¹⁴ for Se and by Maschke¹⁵ for Te. In both of these works, extensive comparisons of the calculated to the experimental optical constant were made.

The only attempts to calculate the density of states of the amorphous forms have been that of Kramer and co-workers⁴⁻⁶ for amorphous Se and that of Hartmann and Mahanti⁷ for amorphous Te.

Kramer and co-workers⁴⁻⁶ assumed that the amorphous form retains the same nearest-neighbor arrangement as in the trigonal form. The loss of long-range order was simulated by a Gaussian broadening of the reciprocal-lattice vectors in k space. The pseudopotential coefficients, however, were assumed to be the same as those of the crystalline form. When a Green's-function calculation is performed under these assumptions, the bands in the neighborhood of the gap appear broadened while those far away from it remain sharper. It is not clear whether this broadening is an artifact of the model (e.g., of having assumed no smearing in the pseudopotential factors) or whether intrinsic physical significance should be attributed to it. Nevertheless, this theory was able to explain the optical spectra measured for amorphous Se,⁴ a fact even more remarkable when one considers that the amorphous form contains monoclinic rings excluded from the calculation.

Hartmann and Mahanti,⁷ using a molecular-orbital theory, assumed that the three-atom unit cell of trigonal Te was maintained in the amorphous form and introduced the disorder by distorting the bonds at the ends of the cells. There was no gap at the Fermi level, although the density of states in the "gap region" was small. The only test of the model was for the optical absorption edge: The calculated edge was lower in energy than the measured one. In addition, considerable structure was obtained in the calculated density of valence states.

IV. OPTICAL AND ELECTRICAL PROPERTIES

The difference in the optical and electrical properties of the amorphous and crystalline forms of Se and Te, as recently reviewed by Stuke¹ and Adler,³ suggests that the electronic spectra of the two forms differ significantly. The optical spectra of the amorphous forms show considerably less structure than their corresponding trigonal forms. The ϵ_2 spectrum of amorphous Se has two broad peaks, at 4 and 8 eV,^{1,25} while amorphous Te has one broad strong peak at 3.5 eV with a second weak peak at 7 eV.²⁶ The zero-frequency dielectric constant increases by 12 and 40%, respectively, for Se and Te upon forming the amorphous

phase. This has been interpreted as representing a strengthening of the bonding within the chains at the expense of the bonding between the chains.¹ Such effects, we expect, are signaling considerable differences in the density of valence states of the amorphous and crystalline forms, such as were found in GeTe.²⁷

The optical absorption from the 3d bands in Se and Te has been measured by Cardona *et al.*²⁸ and by Sonntag *et al.*²⁹ The absorption spectra for amorphous and crystalline Se were identical, indicating no major differences in the conduction bands of the two forms. However, it is not clear whether such absorptions are due to one-electron transitions into the conduction band or are affected by Coulomb interaction in the final state (excitonic effects). Comparisons of positions of these absorption peaks to the positions of the corresponding core levels determined with x-ray photoemission spectroscopy (XPS) can be helpful in determining the nature of the absorption process.

V. EXPERIMENTAL

The samples were prepared by dc sputtering in a high-purity-argon atmosphere at 40×10^{-3} Torr. A base pressure of 5×10^{-6} Torr was maintained during sputtering with a turbomolecular pump. To obtain the amorphous form of Se the substrate was held at room temperature. To obtain the trigonal form of Se the substrate was held at 70 °C during deposition; afterwards it was held at 100 °C for 20 min, and at 130 °C for 5 min, and then brought back to room temperature. The work of Champness and Hoffmann³⁰ has shown that films heated from room temperature to 130 °C crystallize in about 5 min. The size of the crystallites was not measured; our results must thus be qualified since work on single crystals may produce even sharper structure than that reported here. The amorphous form of Te was obtained by depositing onto a substrate held at 125 °K, while the crystalline form was obtained by depositing onto a substrate at room temperature.³¹

Immediately after sputtering, the samples were inserted without breaking the vacuum into the analyzing chamber at a pressure better than 5×10^{-10} Torr. The uv spectra were measured first, and then the x-ray spectra. The x-ray spectra of Se showed no trace of contamination from either carbon or oxygen, the lower limit of detectability estimated to be 3 at.%. Similar curves were found using the He II line ($h\nu = 40.8$ eV) further confirming the lack of surface contamination.

For the Te film deposited at $T_s = 150$ °K, a large oxygen peak was observed. This peak went away when the sample was heated to room temperature, suggesting that the oxygen was in water that had condensed on the surface of the films. This made

it impossible to determine the density of valence states with uv photoemission with the sample at low temperatures. The water condensed on the films deposited at low temperatures did not, however, seem to hinder our x-ray measurements.

The measurements were performed with a Vacuum Generators ESCA III system fitted with an Al x-ray source and a differentially pumped gas discharge lamp, where the He used provided lines at 21.2 eV (He I) and 40.8 eV (He II). The resolution of x-ray data for the valence bands, including the linewidth of the excitation source, was 1.5 eV and for the more intensely emitting core levels, 1.2 eV. The resolution of the uv data taken with the 21.2-eV line was 0.1 eV and with the 40.8-eV line, 0.3 eV.

VI. RESULTS

Shown in Figs. 1 and 2 are the raw photoemission curves for the amorphous and trigonal forms of Se, respectively, for the 21.2-, 40.8-, and 1486.6-eV excitation energies. In these figures, the zero scale was positioned at the sharp onset obtained from the 21.2-eV line. The less well resolved emission curves obtained with the He II and AlK spectra were then positioned to make their peak positions match those of the 21.2-eV data. The core levels determined from the x-ray photoemission reported in Table I were referred to the zero determined in this way. The curves for the three modes of excitation are seen to be

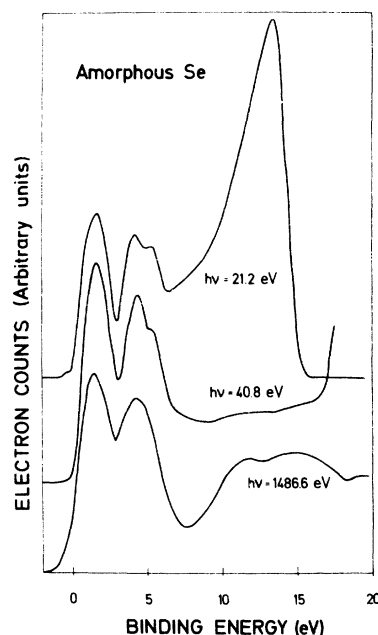


FIG. 1. Raw photoemission data from amorphous Se obtained with photon excitation energies of 21.2, 40.8, and 1486.6 eV.

TABLE I. Core levels of Te and Se (in eV) found in this and other work. Energies in our work are measured with respect to the top of the valence band and are estimated to be the same for the amorphous and the crystalline forms.

Level	$3d_{5/2}$	$3d_{3/2}$	$3p_{3/2}$	$3p_{1/2}$	$3s$
Se ^a	54.64	55.47	160.7	166.47	229.6
Se ^b	56.7		161.9	168.2	231.5

Level	$4d_{5/2}$	$4d_{3/2}$	$4s$	$3d_{5/2}$	$3d_{3/2}$	$3p_{3/2}$	$3p_{1/2}$	$3s$
Te ^a	40.5	41.95	165.5	572.55	583.34	819.8	870.6	1004.9
Te ^b		35.8	168.3	572.1	582.5	818.7	869.7	1006.0
Te ^c	40.31	41.5						

^aThis work.

^cFrom Ref. 16.

^bFrom Ref. 19.

quite similar. The only major differences arise in the large secondary tail in the photoemission of the 21.2-eV photons. The structure in the first two peaks is less well resolved in the x-ray photoemission owing to the poorer resolution (~ 1.5 eV). The emission curve from amorphous Se with the 21.2-eV photon excitation is in excellent agreement with that determined by Nielsen.²³ We also do not see the peak produced by s -like bands. There are hints of this peak in the 40.8-eV emission curves, but these bands are clearly better resolved in the x-ray emission. The fact that all curves yield similar structure indicates that they are free of the effects of matrix elements and surface contamination; they thus yield the density of bulk valence states. Within the resolution of the

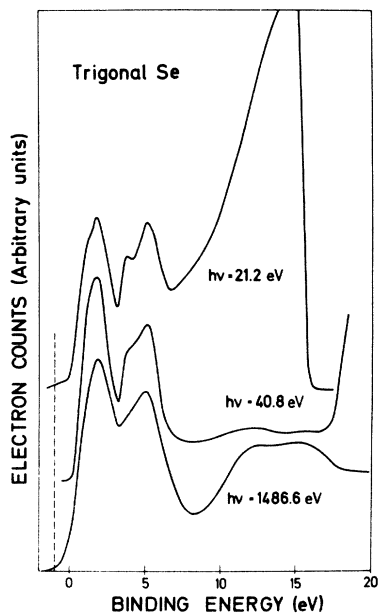


FIG. 2. Raw photoemission data from crystalline Se obtained with photon excitation energies of 21.2, 40.8, and 1486.6 eV.

x-ray measurements there are essentially no differences between the density of valence states for the two forms. Similar observations have been made for AlSb.³² With the improved resolution of the uv emission, the differences in the top valence bands, particularly the lower bonding p set, become more pronounced. In Fig. 3 the uv photoemission data with 21.2-eV photons for the two structural forms of Se are plotted on an expanded scale so that comparisons between them can be more easily made. In particular, the triplet structure that appears in the 2-eV peak of the crystalline material can be clearly observed. Combining the x-ray photoemission, which resolves the lower s band with the uv data, which has better resolution in the upper two bands, and correcting for secondary electrons,²⁷ we derive a composite density of states shown in Fig. 4. The dotted line indicates the region where the two sets of data have been matched. Also plotted on this figure is the density of valence states calculated by Kramer *et al.*⁵ for the amorphous form.

In Fig. 5 we present the photoemission data for trigonal Te. The x-ray emission data are similar to those found by Pollak *et al.*¹⁶ The emission from the 40.8-eV line does not appear to give a density of states characteristic of the bulk: The peak with 4.5-eV binding energy is stronger than in the other measurements and oxygen contamination strengthens this peak even further. We thus believe that such spectra arise from surface contamination with oxygen which gives significant contributions to the emissions curves when the escape depth of the electrons becomes small. The agreement of the 21.2-eV emission curve with that determined from x rays (Fig. 6) suggests that the effects of contamination are less here (the escape

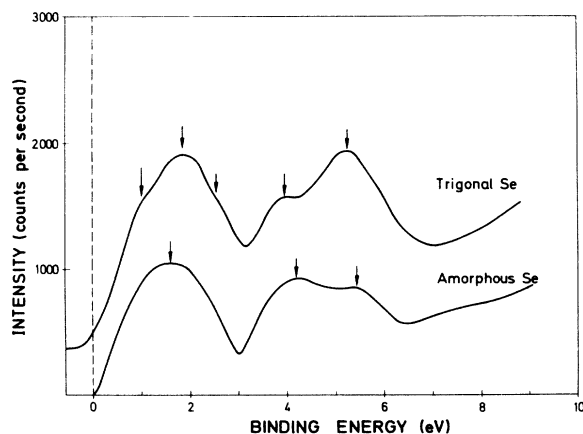


FIG. 3. Comparison of the raw emission data from amorphous and crystalline Se obtained with $h\nu = 21.2$ eV. This figure shows clearly the triplet structure which appears in the 2-eV peak when the material crystallizes.

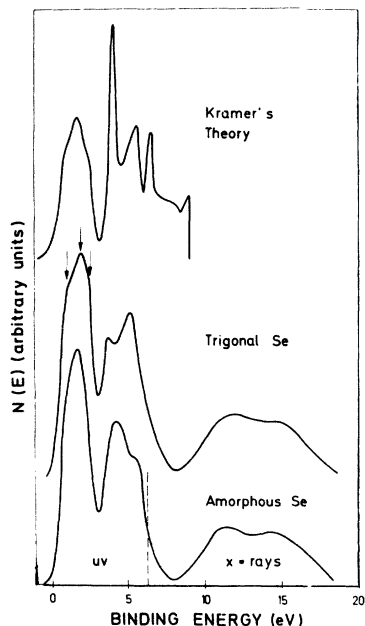


FIG. 4. Composite density of valence states of amorphous and crystalline Se. The upper curve shows the density of states calculated by Kramer *et al.* (Ref. 5).

depth for emitted valence electrons is larger in this case). Combining the 21.2-eV and the x-ray data, we deduce a composite density of states for crystalline Te as shown in Fig. 7.

As already mentioned, water condensation prevented us from obtaining uv photoemission data on the amorphous form of Te which must be kept at a low temperature (amorphous Te crystallizes

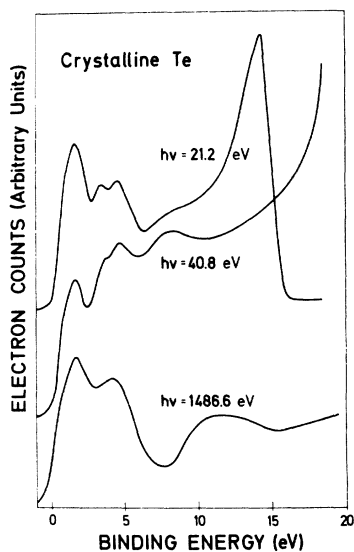


FIG. 5. Raw emission data from trigonal Te obtained with photon excitation energies of 21.2, 40.8, and 1486.6 eV.

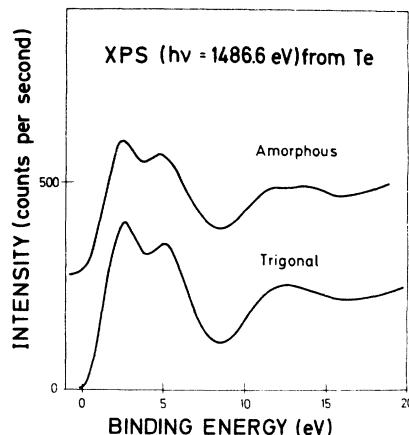


FIG. 6. Raw x-ray photoemission data from amorphous and trigonal Te.

when the sample is brought to room temperature). However, the x-ray data, shown in Fig. 6, were apparently unaffected by water condensation. Within the resolution of the XPS measurements we see essentially no differences between the density of valence states of the two structural forms.

The characteristic energy loss spectra following the Se $3d$ level and the Te $3p_{3/2}$ for the amorphous and trigonal forms are shown in Figs. 8 and 9, respectively. For both curves, the peak at zero binding energy corresponds to electrons that have escaped the sample without undergoing inelastic collisions. The resolution of the loss curves is given by essentially the widths of these primary peaks. The loss energy was measured with respect to the center of these primary peaks. Since the positions of the Fermi levels of the structural modifications were different, the primary peaks were aligned so as to fall at the same position on the abscissa axis. The arrows indicate the maxima in the loss curves, i. e., the plasmon frequencies.

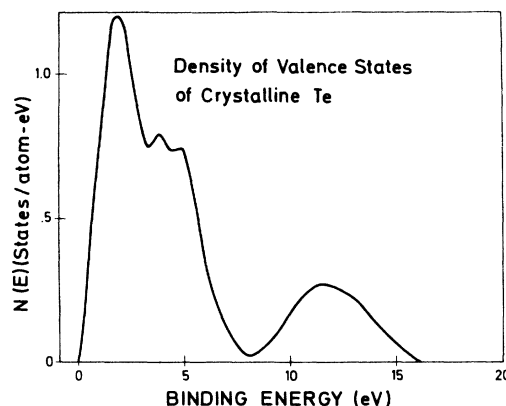


FIG. 7. Composite density of valence states of crystalline Te.

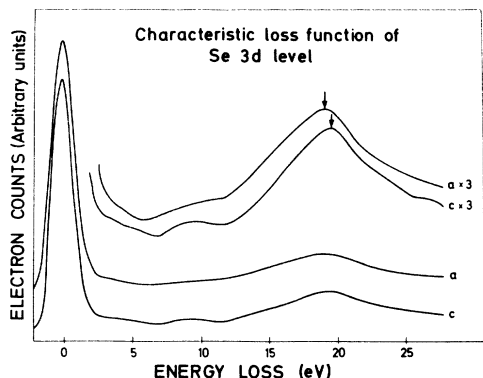


FIG. 8. Loss spectra following the Se $3d$ level in the amorphous and crystalline forms.

They occur in Se at 19.2 ± 0.2 and 19.8 ± 0.2 eV, and in Te at 17.4 ± 0.5 and 17.5 ± 0.5 eV, for the amorphous and crystalline forms, respectively. The absence of any sharp structure in the loss peaks emphasizes the fact that secondary electrons can add no structure to the deduced densities of states.

VII. DISCUSSION

Se

Referring to Fig. 4, we see that the valence bands of Se exhibit three main peaks for both structural modifications. The lowest peak, centered at 13 eV and associated with the Se s bands, is well separated from the upper peaks. Its 9-eV width indicates that s orbitals band significantly. The peak at 5 eV is associated with the bonding p band, and the peak at 2 eV with the lone-pair orbitals. The top two peaks in the data shown in Fig. 4 for the valence bands of the amorphous form are in excellent agreement with those found by Nielsen.²³ As already mentioned, the lower s band was not seen in either this or Nielsen's work. Nielsen suggested that matrix elements could not explain its absence. We suggest that final density-of-states effects are responsible for the absence of the observed s bands. By examining the density of conduction states calculated by Kramer *et al.*⁵ we find that a minimum occurs 7 eV above the top of the valence band. Thus, the electrons emitted from the lower s set at 13 eV by the 21.2 electrons fall at 8 eV above the top of the valence band, close to this minimum. Also, the width of this lower band (~ 9 eV) makes it difficult to see in the rapidly rising contribution from the secondaries.

The band structure calculated by Sandrock¹⁴ seems to describe the over-all features of the density of valence states remarkably well. He finds the lone-pair bands, the bonding p bands, and the s bands to be centered at 1.7, 5.3, and 12.4 eV below the top of the valence band, respec-

tively. The calculated widths of the corresponding bands are 2.8, 5, and 7.5 eV. Inspection of Fig. 4 shows that all of these numbers are in excellent agreement with experiment, and similar agreement with pseudopotential theory was found by Grobman and Eastman³³ in their measurements of the valence bands of Ge and Si. Of particular interest is that the position and width of the lowest s bands are accurately described by pseudopotential calculation, in spite of the fact that it is not expected to be accurate far from the Fermi level. In contrast, the s valence bands measured for the lead chalcogenides disagree strongly with the results of pseudopotential calculations,^{17,18} a fact which, in view of the present results, is probably due to the ionicity of these materials.

The primary difference between the density of states of the two structural forms is in the top two p -like bands. The lone-pair band in the amorphous form is slightly asymmetric while that of the crystal shows a distorted top with a triplet substructure, in good agreement with that calculated by Kramer and co-workers.⁴⁻⁶ The largest differences occur in the bonding p band. This peak in the amorphous form has a shoulder on the high-energy site at ~ 5.5 eV while that of the crystal has a minor peak on the high-energy site at ~ 3.5 eV. The total width of the bonding p band is about 1.5 eV narrower than calculated. However, the over-all agreement of the calculations of Kramer and co-workers⁴⁻⁶ to the density of states of the trigonal form is seen to be good. This agreement would improve if the theoretical curves were to be broadened more.

The better agreement of the amorphous density of states calculated by Kramer and co-workers⁴⁻⁶ with our experimental trigonal density of states is not very surprising. Lifetime broadening from electron-electron and electron-phonon interactions likely produces as much smearing as the positional disorder of Kramer and co-workers.⁴⁻⁶ The

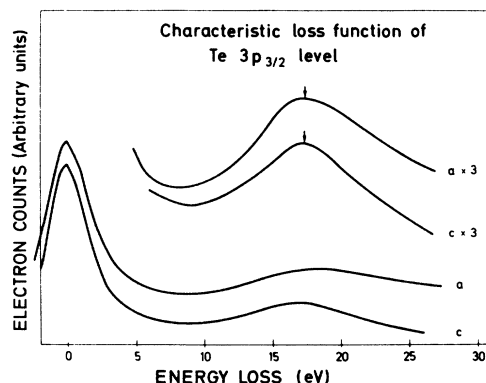


FIG. 9. Loss spectra following the $3p_{3/2}$ level in the amorphous and crystalline forms of Te.

poorer fit of the experimentally determined density of states of the amorphous form is probably related to dissimilarities in the structures of the two forms. Use of a more appropriate structural model for the amorphous form appears to be necessary to bring the calculation into agreement with experiment.

It is interesting to note that the valence bands calculated by Sandrock¹⁴ in the $k_x = \pm \pi/c$ basal planes are very flat and represent rather well our photoemission results for the amorphous form. In these planes we find an upper "lone-pair" set of three bands, nearly degenerate at the *A* point (edge of the zone along *c* axis) and spreading only slightly into a triplet away from *A*. The next band, about 2 eV deeper, is twofold degenerate at *A* and barely splits away from *A*. A splitting of 2 eV separates these bands from the lowest *p*-like band. Thus the contribution to the density of states from these planes produces a bonding *p* band split into two peaks with the strengths 2:1, similar to the experimentally observed peak.

Te

The experimental density of valence states of Te, shown in Fig. 7, is similar to that found for Se. In agreement with qualitative theoretical predictions,¹³⁻¹⁵ the primary difference is that the lone-pair and bonding *p* bands are not as well separated as they are in Se. The lowest *s* bands peak at about 11.4 eV and are about 5 eV wide. According to the pseudopotential calculation of Maschke,^{15,34} the lower *s* bands extend from 10 to 14 eV below the top of the valence band, in good agreement with the present measurements. Again it is surprising that the pseudopotential method has been able to determine accurately the position of a peak so far away from the Fermi level. The ratio of the total strength of the *p* bands to that of the *s* bands is larger than the corresponding ratio in Se. It has been found that with decreasing atomic number, the lower portions of the valence bands become more pronounced relative to the upper portions in the x-ray photoemission. The lone-pair band peaks strongly at about 2-eV binding energy. Its shape is similar to the corresponding peak observed in trigonal Se. The bonding *p* band presumably broadens to overlap with the lone-pair band. The total width of the two sets of *p* bands is observed to be ~6 eV, compared to the 3.5-eV width calculated by Maschke. The experimental curve shows considerably less structure than the density of states calculated by Hartmann and Mahanti for the amorphous form.

In a crystalline solid the dielectric constant is usually computed on the basis of direct *k*-conserving transitions. In the case of Te, however, the *p*-like conduction bands as a function of *k* are

extremely flat¹⁵ and the distinction between direct and indirect transitions may lose meaning. We therefore tried to compute the ϵ_2 spectrum of crystalline Te by assuming constant dipole matrix elements and a δ -function-like density of conduction states. The "average" ϵ_2 should then be given by

$$\epsilon_2(\nu) \propto N_v (E_0 - \hbar\nu)/\nu^2, \quad (1)$$

where the E_0 is the band gap chosen to have the value 1.2 eV, and N_v is the density of valence states. The result obtained by replacing into Eq. (1) the density of states of Fig. 7 is shown in Fig. 10 and compared with the average experimental ϵ_2 . The good agreement shows that our model, the experimental valence bands obtained from photoemission and a sharp conduction band, provides a good representation of the average dielectric constant of crystalline Te.

Core Levels

The positions of the core levels listed in Table I are in disagreement with those reported by Bearden and Burr.¹⁹ In the present work the effects of charging and uncertainties in the Fermi levels have been removed by measuring all levels with respect to the top of the valence band. For amorphous Se this was particularly important since the charging effects appear to lead to an additional shift of about 1 eV compared to the crystalline form. If we measure our amorphous Se with respect to the Fermi energy of our spectrometer we still obtain results that are 1 eV less in binding energy than those reported by Bearden and Burr.¹⁹ For the amorphous and crystalline forms, there were no differences in the positions of the

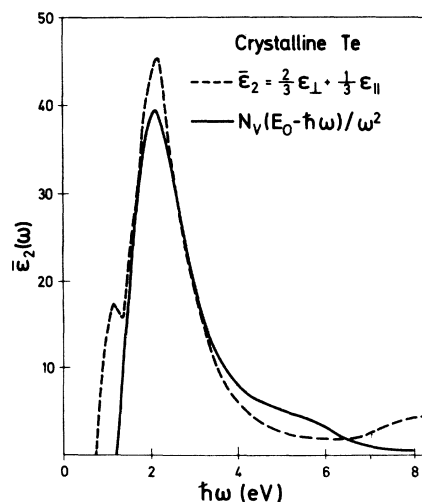


FIG. 10. Average experimental ϵ_2 spectrum of trigonal Te (Ref. 26) compared with that determined from the experimental density of valence states.

core levels within our 0.2 eV accuracy, provided one refers them to the top of the valence band.

Absorption from Core Levels

The absorption spectra produced by transitions from core levels to conduction bands have recently received considerable attention because of the availability of synchrotron radiation as a spectroscopic source. It is of interest to determine whether the peaks in these spectra occur at energies which are the sum of the binding energy of the core levels determined with photoemission plus the energy at which the peak in the density of conduction states occurs. The main peak at the onset of the $3d$ absorption of Se (either amorphous or crystalline) has a shoulder at 55.2 eV, followed by a peak at 56.2 eV. We have found the corresponding core level to be 54.6 eV below the top of the valence band. Adding to this energy the energy at which the first peak in the density of conduction states occurs (3 eV), we obtain 57.6 eV, an energy much higher than any of the observed absorption structure. This discrepancy appears even more dramatically in Fig. 11. We have represented in this figure the calculated density of valence and conduction states, the experimental density of valence states, and the "density of conduction states" obtained from the synchrotron radiation experiments.²⁸ The origin of energies has been fixed for the synchrotron data by using as the initial energy for the absorption process the $3d$ core levels of x-ray photoemission measured with respect to the "lone-pair" peak of the uv valence band photoemission.

The density of conduction states obtained in the synchrotron experiments, or actually the absorption coefficient, peaks about 1 eV below the calculated density of states and has a long tail ex-

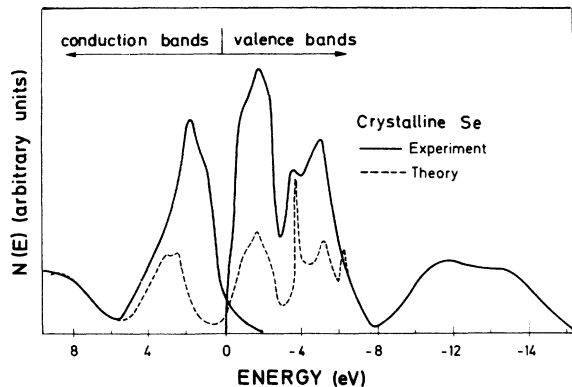


FIG. 11. Density of valence and conduction states of Se determined from the photoemission data in this work and the optical absorption data of Ref. 28, compared with the theoretical density of states of Kramer *et al.* (Ref. 5).

TABLE II. Plasma energies (in eV) in amorphous (*a*) and crystalline (*c*) Se and Te.

	ESCA	Optical	Energy loss	$h\omega_p$ (free electron)
<i>c</i> -Se	19.9	19.9 ^a	19.9 ^a	17.4
<i>a</i> -Se	19.3	18.9 ^b	18.8 ^c 17.0 ^c	16.5
<i>c</i> -Te	17.4	17.3 ^a	17.3 ^a 17.9 ^d	14.9
<i>a</i> -Te	17.5			

^aFrom Ref. 36 (average of the parallel and twice the perpendicular electric field configuration).

^bReference 25.

^cReference 37.

^dReference 39.

tending to ~ 2 eV, deep into the valence band. Above 3 eV this density of states agrees again with the calculated one.

Because of the reliability of the calculated density of states, based in part on the good agreement with the experimental density of valence states, we believe to have obtained here evidence for final-state interaction in the absorption spectrum. In fact, these results are quite similar to those reported for the $2p$ absorption of Si.^{35,36} The one-electron density of conduction states is enhanced at the edge and pulled down in energy by the Coulomb interaction in the final state.

A similar situation, although less clear, arises in Te. The first absorption peak occurs at 40.95 eV, an energy which is somewhat smaller than the sum of the binding energy of the $4d_{5/2}$ level (40.5 eV) and the energy of the peak on the density of conduction states (~ 1 eV).

Energy Loss Function

The data obtained from the energy loss curves are summarized in Table II. The energy loss functions of Se (Fig. 8) peak at 19.3 and 19.9 eV for the amorphous and crystalline forms, respectively. The results are consistent with the known 5-10% difference between the densities of the amorphous and crystalline phases. The plasma frequency of the crystalline form is in good agreement with that found by Bammes *et al.*,³⁷ while that of the amorphous form is 0.4 eV higher than that found by Vasko²⁵ from optical data (18.9 eV). Robins³⁸ found in electron energy loss experiments a plasma frequency of 18.8 eV for amorphous Se. A small peak at 5.4 eV seen in some of these experiments at ~ 5 eV was not observed in our work. We observed instead a slight structure around 10 eV, also seen in Ref. 37, which could bear some relationship to the zero in ϵ_1 , reported by Vasko²⁵ at this energy. The energy of the main loss peak in Fig. 8 (~ 19.9 eV for crystalline Se) represents the plasma frequency of this material.

This frequency is far from the value of 17.4 eV calculated for a free-electron gas in crystalline Se. As discussed by Pines,³⁹ an increase in the plasma energy is expected when there exists appreciable oscillator strength between transitions with frequencies slightly below that of the free-electron plasmon frequency. The s bands ranging from 12 to 19 eV suggest that such an oscillator strength may exist.

For Te we obtain from our measurements a plasma frequency of 17.4 eV for the two forms. The peak is too broad to distinguish between amorphous and crystalline, and thus we are not able to see any appreciable density difference between the amorphous and crystalline forms. The

calculated free-electron value, 14.9 eV, is also smaller than the measured one, which again is attributable to an appreciable oscillator strength lying at frequencies slightly below the free-electron plasma frequencies. The value of 17.9 eV was reported by Leder⁴⁰ for the plasma frequency of crystalline Te.

ACKNOWLEDGMENTS

Valuable discussions with Professor J. Stuke and Dr. B. Kramer, Dr. D. W. Langer, Dr. K. Maschke, Dr. H. Overhof, Dr. P. Thomas, and Dr. G. Zimmerer are gratefully acknowledged. The measurements were performed with the able assistance of G. Krutina.

- ¹J. Stuke, *J. Non-Cryst. Solids* **4**, 1 (1970).
²J. Stuke, *The Physics of Selenium and Tellurium* (Pergamon, Oxford, England, 1969), p. 3.
³D. Adler, *Crit. Rev. Solid State Sci.* **2**, 317 (1971).
⁴B. Kramer, K. Maschke, P. Thomas, and J. Treusch, *Phys. Rev. Lett.* **25**, 1020 (1970).
⁵B. Kramer, K. Maschke, and P. Thomas, *J. Phys. Suppl.* **33**, 157 (xxxx).
⁶K. Maschke and P. Thomas, *Phys. Status Solidi* **b41**, 743 (1970).
⁷W. M. Hartmann and S. D. Mahanti, *J. Non.-Cryst. Solids* **8-10**, 633 (1972).
⁸J. R. Reitz, *Phys. Rev.* **105**, 1233 (1957).
⁹S. Tutihasi and I. Chen., *Phys. Rev.* **158**, 623 (1967).
¹⁰R. E. Beisner, *Phys. Rev.* **145**, 479 (1966).
¹¹D. T. Olechna and R. S. Knox, *Phys. Rev.* **140**, 986 (1968).
¹²M. Picard and M. Huhn, *Phys. Status Solidi* **b23**, 563 (1967).
¹³J. Treusch and R. Sandrock, *Phys. Status Solidi* **b16**, 487 (1966).
¹⁴R. Sandrock, *Phys. Rev.* **169**, 642 (1968).
¹⁵K. Maschke, *Phys. Status Solidi* **b47**, 511 (1971).
¹⁶R. A. Pollak, S. Kowalczyk, L. Ley, and D. A. Shirley, *Phys. Rev. Lett.* **29**, 274 (1972).
¹⁷M. Cardona, D. W. Langer, N. J. Shevchik, and J. Tejada, *Phys. Status Solidi* **b58**, 127 (1973).
¹⁸F. R. McFeely, S. Kowalczyk, L. Ley, and R. A. Pollak (unpublished).
¹⁹J. A. Bearden and A. F. Burr, *Rev. Mod. Phys.* **39**, 125 (1967).
²⁰L. D. Laude, B. Fitton, and M. Anderegg, *Phys. Rev. Lett.* **26**, 637 (1971).
²¹L. D. Laude, B. Fitton, B. Kramer, and K. Maschke, *Phys. Rev. Lett.* **27**, 1053 (1971).
²²L. D. Laude and B. Fitton, *J. Non-Cryst. Solids* **8-10**, 971 (1972).
²³P. Nielsen, *Phys. Rev. B* **6**, 3739 (1972).
²⁴A. Koma, O. Mizuno, S. Tanaka, *Phys. Status Solidi* **b46**, 225 (1971).
²⁵A. Vasko, *J. Non-Cryst. Solids* **3**, 225 (1970).
²⁶S. Tutihasi, G. G. Roberts, R. C. Keezer, and R. E. Drews, *Phys. Rev.* **177**, 1043 (1969).
²⁷N. J. Shevchik, J. Tejada, D. W. Langer, and M. Cardona, *Phys. Status Solidi* **b57**, 245 (1973).
²⁸M. Cardona, W. Gudat, B. Sonntag, and P. Yu, *Proceedings of the Tenth International Conference on the Physics of Semiconductors* (U. S. Atomic Energy Commission, Oak Ridge, Tenn., 1970), p. 209.
²⁹B. Sonntag, T. Tuomi, and G. Zimmerer, *Eleventh International Conference on the Physics of Semiconductors, Warsaw, 1972* (Polish Scientific Publ., Warsaw, 1972); also private communication.
³⁰C. H. Champness and R. H. Hoffmann, *J. Non-Cryst. Solids* **4**, 138 (1970).
³¹H. Keller and J. Stuke, *Phys. Status Solidi* **b8**, 831 (1965).
³²N. J. Shevchik, J. Tejada, C. M. Penchina, and M. Cardona, *Solid State Commun.* **11**, 1619 (1972).
³³W. D. Grobman and D. E. Eastman, *Phys. Rev. Lett.* **29**, 1508 (1972).
³⁴K. Maschke (private communication).
³⁵C. Gähwiller and F. C. Brown, *Proceedings of the International Conference on the Physics of Semiconductors, Cambridge, Mass., 1970* (U. S. Atomic Energy Commission, Oak Ridge, Tenn., 1970), p. 213.
³⁶M. Altarelli and D. L. Dexter, *Phys. Rev. Lett.* **29**, 1100 (1972).
³⁷P. Bammes, R. Klucker, E. E. Koch, and T. Tuomi, *Phys. Status Solidi* **b49**, 561 (1972).
³⁸J. L. Robins, *Proc. Phys. Soc. (London)* **79**, 119 (1962).
³⁹D. Pines, *Rev. Mod. Phys.* **28**, 184 (1956).
⁴⁰L. B. Leder, *Phys. Rev.* **103**, 1721 (1956).